Drug Target Insights 2025 | DOI: 10.33393/dti.2025.3368 | Thakkar et al

Supplementary file

Withania somnifera root extract (LongeFera™) confers beneficial effects on health and lifespan of the model worm *Caenorhabditis elegans*

Nidhi Thakkar[1#], Gemini Gajera[1#], Dilip Mehta[2], Sujit Nair[2], Vijay Kothari[1*]

[1] Institute of Science, Nirma University, Ahmedabad-382481, India
[2]Phytoveda Pvt. Ltd., Mumbai-400022, India
*Correspondence: vijay.kothari@nirmauni.ac.in
[#]Contributed equally

Supplementary Materials list

Table S1. Quantification of extracted RNA, library, and insert size

Sr. no.	Sample	Quantification of extracted RNA			Library quantification and insert size analysis	
		OD_{260}/OD_{280}	OD_{260}/OD_{230}	RIN value	ng/µL	Insert size (bp)
1	Control	1.9	2	8.9	39.4	321
2	Experimental	1.8	0	9.6	35.6	314

Table S2. Temperature profile for RT-PCR assay

Temperature (°C)	Time (s)	Remarks
PCR cycles (45 cycles)		
95	15	Denaturation temperature
59	60	Annealing temperature
Melt curve stage		
95	15	
60	60	
95	15	

Table S3. Node degree score of the upregulated genes in *W. somnifera*-exposed *C. elegans*

Sr. No.	Gene ID/ symbol	Node Degree
1	*cpg-3*	10
2	F22B3.4	9
3	*cpg-2*	9
4	*perm-2*	9
5	*vit-2*	8
6	*vit-5*	8
7	*vit-6*	8
8	W03F11.1	7
9	Y62H9A.3	7
10	*clec-87*	5
11	*rmd-1*	4
12	F15E11.12	1
13	F15E11.15	1

Rest 2 genes with node degree score ‘zero’ are not listed.

Table S4. Node degree score of the downregulated genes in *W. somnifera*-exposed *C. elegans*

Sr. No.	Gene ID/ symbol	Node Degree
1	*sqt-1*	8
2	*unc-52*	8
3	*col-169*	6
4	*dpy-13*	6
5	*dpy-4*	6
6	*let-805*	6
7	*mlt-11*	6
8	*ttn-1*	6
9	*col-17*	5
10	*col-41*	5
11	*ketn-1*	5
12	*lpr-3*	5
13	*col-109*	4
14	*dig-1*	4
15	*fbn-1*	4
16	*sqt-3*	4
17	*unc-68*	4
18	*vab-10*	4
19	H03E18.1	3
20	Y65B4BL.1	2
21	*cdh-12*	2
22	*nep-17*	2
23	F28B4.3	1

Rest 6 genes with node degree score ‘zero’ are not listed.

Table S5. Functions of human genes which are homologous to the differently expressed genes in extract-treated worms

Sr. No.	Gene symbol	Function
1	GFPT1	Glutamine--fructose-6-phosphate aminotransferase [isomerizing] 1; Controls the flux of glucose into the hexosamine pathway. Most likely involved in regulating the availability of precursors for N- and O-linked glycosylation of proteins. Regulates the circadian expression of clock genes ARNTL/BMAL1 and CRY1.
2	RYR2	Ryanodine receptor 2; Calcium channel that mediates the release of Ca^{2+} from the sarcoplasmic reticulum into the cytosol and thereby plays a key role in triggering cardiac muscle contraction.
3	COL6A5	Collagen alpha-5(VI) chain; Collagen VI acts as a cell-binding protein.
4	COL6A5	Collagen alpha-5(VI) chain; Collagen VI acts as a cell-binding protein.
5	COL6A5	Collagen alpha-5(VI) chain; Collagen VI acts as a cell-binding protein.
6	RMDN1	Regulator of microtubule dynamics 1.
7	COL12A1	Collagen alpha-1(XII) chain; Type XII collagen interacts with type I collagen-containing fibrils, the COL1 domain could be associated with the surface of the fibrils, and the COL2 and NC3 domains may be localized in the perifibrillar matrix.
8	COL6A6	Collagen alpha-6(VI) chain; Collagen VI acts as a cell-binding protein.
9	SLC17A6	Vesicular glutamate transporter 2; Mediates the uptake of glutamate into synaptic vesicles at presynaptic nerve terminals of excitatory neural cells. May also mediate the transport of inorganic phosphate. Belongs to the major facilitator superfamily. Sodium/anion cotransporter family. VGLUT subfamily.
10	MLF2	Myeloid leukemia factor 2.
11	ECE2-2	EEF1AKMT4-ECE2 read through transcript protein; Converts big endothelin-1 to endothelin-1. May also have methyltransferase activity (By similarity). May play a role in amyloid- beta processing (By similarity); In the C-terminal section; belongs to the peptidase M13 family.
12	MACF1	Microtubule-actin cross-linking factor 1, isoforms 1/2/3/5; [Isoform 2]: F-actin-binding protein which plays a role in cross-linking actin to other cytoskeletal proteins and also binds to microtubules.
13	ADH4	All-trans-retinol dehydrogenase [$NAD^{(+)}$] ADH4; Catalyzes the NAD-dependent oxidation of either all-trans- retinol or 9-cis-retinol.
14	COL25A1	Collagen-like Alzheimer amyloid plaque component; Inhibits fibrillization of amyloid-beta peptide during the elongation phase. Has also been shown to assemble amyloid fibrils into protease-resistant aggregates. Binds heparin.
15	HSPG2	Heparan sulfate proteoglycan 2.
16	COL6A1	Collagen alpha-1(VI) chain; Collagen VI acts as a cell-binding protein.

(Source: https://version-12-0.string-db.org/cgi/cooccurrence?networkId=bBZLpbKyQ4Xt)

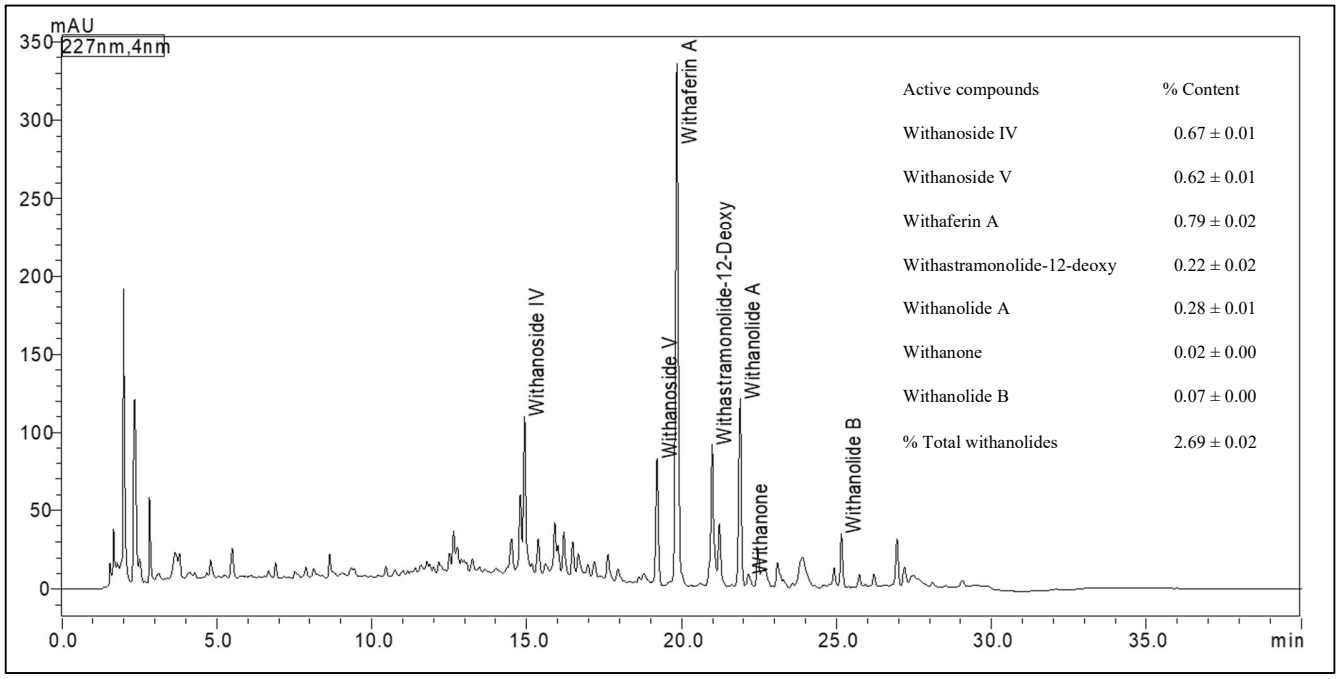

Figure S1. HPLC profile and marker identification in *W. somnifera* root extract

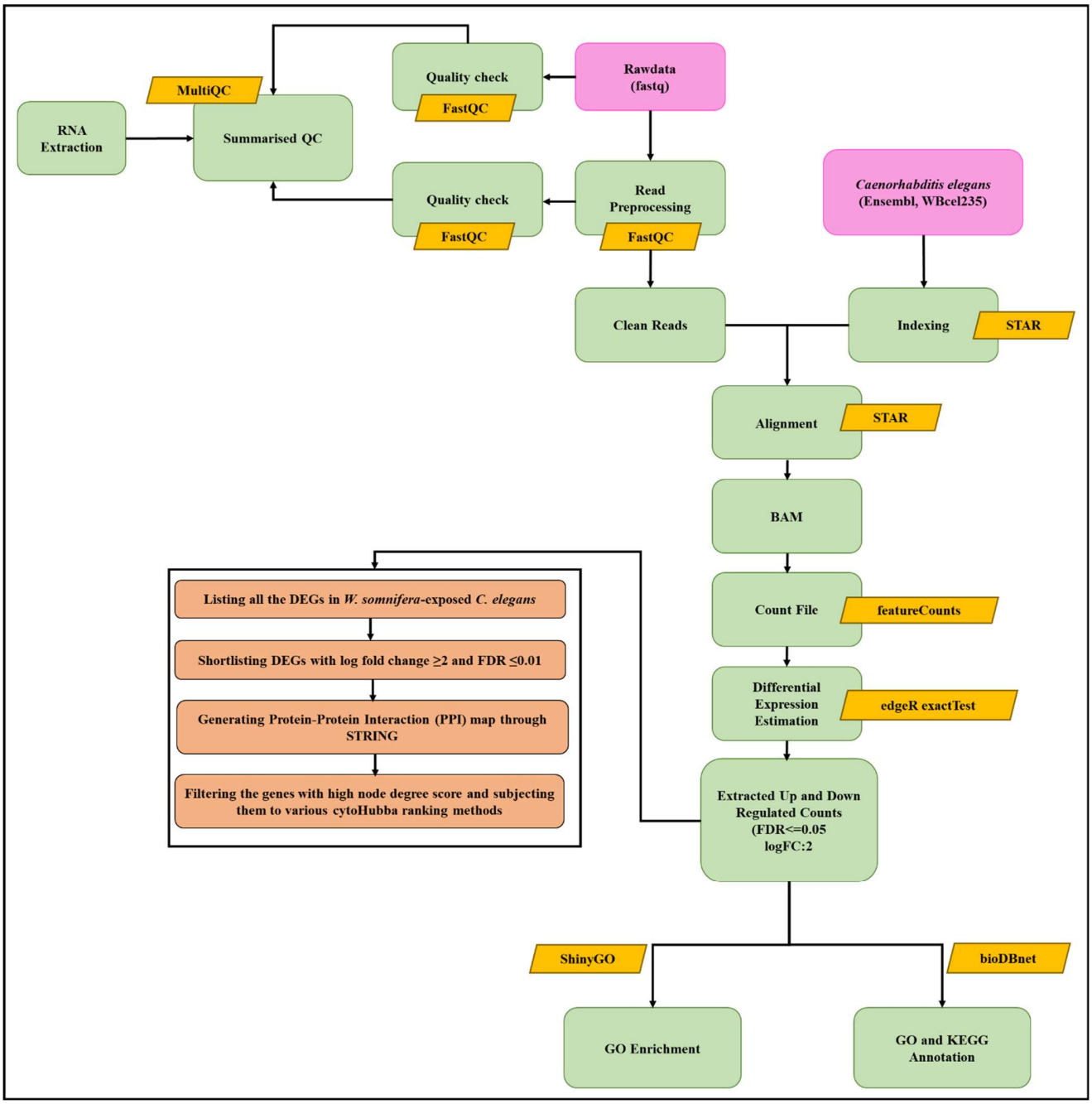

Figure S2. A schematic presentation of the workflow for whole transcriptome and network analysis of extract-treated worms

DEG: Differentially Expressed Genes; FDR: False Discovery Rate; log FC: log Fold Change; GO: Gene Ontology (GO); KEGG: Kyoto Encyclopedia of Genes and Genomes

Methodological details pertaining to workflow depicted in Figure S2:

RNA Extraction

Worm RNA was extracted by the Trizol (Invitrogen Bioservices, Mumbai, India; 343909) method. RNA was precipitated using isopropanol, followed by washing with ethanol (75%), and then the RNA was suspended in nuclease-free water. RNA thus extracted was quantified on Qubit 4.0 fluorimeter (Thermofisher, Mumbai, India; Q33238) making use of an RNA HS assay kit (Thermofisher; Q32851) as per the manufacturer's protocol. Concentration and purity of RNA were assessed on Nanodrop 1000. RIN (RNA Integrity Number) value was known by assessing the RNA on the TapeStation using HS RNA ScreenTape (Agilent) (Table S1).

Library Preparation

The final libraries prepared using Trueseq standard total RNA (Illumina #15032611) were quantified on a Qubit 4.0 fluorimeter, using a DNA HS assay kit (Thermofisher; Q32851). To determine the insert size of the library, it was queried on Tapestation 4150 (Agilent) using highly sensitive D1000 screentapes (Agilent; 5067-5582). Acquired sizes of both libraries are listed in Table-S1.

Genome Annotation and Functional Analysis

Quality assessment of the raw fastq reads of the sample was achieved using FastQC v.0.11.9 (default parameters). The raw fastq reads were pre-processed using Fastp v.0.20.1, followed by a reassessment of the quality using FastQC. The processed reads were aligned to the STAR indexed *Caenorhabditis elegans* (Ensembl, WBcel235) genome using STAR aligner v 2.7.9a (parameters: --outSAMtype BAM SortedByCoordinate --outSAMunmapped Within --quantMode TranscriptomeSAM --outFilterScoreMinOverLread 0.5 --outFilterMatchNminOverLread 0.5 --outSAMattributes Standard). The rRNA and tRNA features were removed from the GTF file of *C. elegans*. The alignment file (sorted BAM) from individual samples was quantified using featureCounts v. 0.46.1 based on the filtered GTF file to obtain gene counts. These gene counts for *C. elegans* were used as inputs to edgeR with exactTest for differential expression estimation (parameters: dispersion = 0.1). Gene Ontology (GO) and Kyoto Encyclopedia of Genes and Genomes (KEGG) pathway annotation of the samples was performed using bioDBnet. The EdgeR exact Test annotated file was filtered based on adjusted *p*-value (FDR) ≤0.05 and Log Fold Change ± 2. Volcano plots were generated using Enhanced Volcano, and the MA plots were plotted using ggmaplot function of ggpubr R package. Gene set GO enrichment analysis was done using ShinyGO (parameters: Organism: *C. elegans*, FDR≤0.05).

Network Analysis

From among all the differentially expressed genes (DEG) in *W. somnifera*-exposed *C. elegans*, those fulfilling the dual filter criteria of False Discovery Rate (FDR) ≤ 0.01 and log fold change ≥ 2 were selected for further network analysis. A list of such DEG was input into the STRING (v.12) database (Szklarczyk et al., 2019) to create the PPI (Protein–Protein Interaction) network. Members of this PPI network were then arranged in descending order of 'node degree' (a

quantitative indication of connectivity with other proteins or genes), and those above a specified threshold value were forwarded for ranking by the cytoHubba plugin (v.3.9.1) (Chin et al., 2014) of Cytoscape (Shannon et al., 2003). As cytoHubba uses twelve different ranking methods, we considered the DEG top-ranked by a minimum of 6 different methods (50% of the total ranking methods) for further investigation. A separate PPI network of these top-ranked proteins was then generated. The above-described sequence of operations enabled us to end up with a limited number of proteins fulfilling multiple biological and statistical significance criteria simultaneously: (i) FDR ≤ 0.01; (ii) log fold change ≥ 2; (iii) relatively higher node degree; (iv) top-ranking by a minimum of 6 cytoHubba method.

References

Chin, C.H.; Chen, S.H.; Wu, H.H.; Ho, C.W.; Ko, M.T.; Lin, C.Y. cytoHubba: Identifying hub objects and sub-networks from complex interactome. *BMC System Biology*. 2014, 8, S11. DOI: https://doi. org/10.1186/1752-0509-8-S4-S11

Shannon, P.; Markiel, A.; Ozier, O.; Baliga, N.S.; Wang, J.T.; Ramage, D.; Amin, N.; Schwikowski, B.; Ideker, T. Cytoscape: A software environment for integrated models of biomolecular interaction networks. *Genome Research*. 2003, 13, 2498–2504. DOI: https://doi. org/10.1101/gr.;1239303:2498-504.

Szklarczyk, D.; Gable, A.L.; Lyon, D.; Junge, A.; Wyder, S.; Huerta-Cepas, J.; Simonovic, M.; Doncheva, N.T.; Morris, J.H.; Bork, P.; et al. STRING v11: Protein–protein association networks with increased coverage, supporting functional discovery in genome-wide experimental datasets. *Nucleic Acids Research* 2019, 47, D607-13.

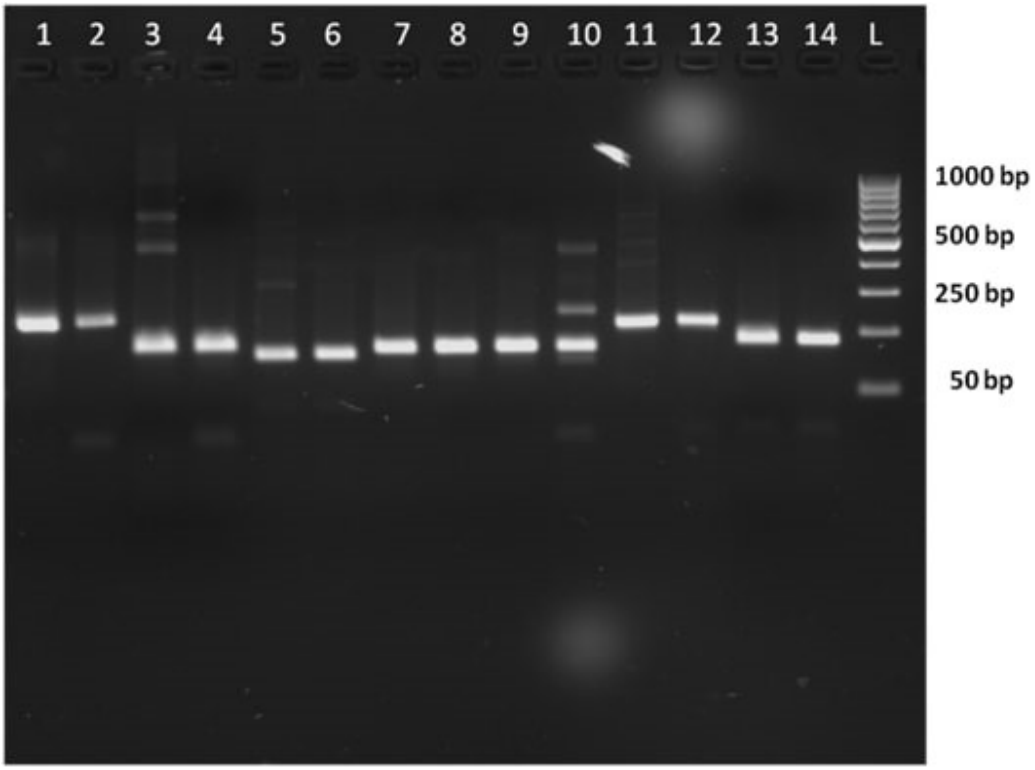

Figure S3. Gel image for primers listed in Table-1 of the main manuscript

Lane 1: *sqt-1* (experimental); Lane 2: *sqt-1* (control); Lane 3: *dpy-4* (experimental); Lane 4: *dpy-4* (control); Lane 5: *col-17* (experimental); Lane 6: *col-17* (control); Lane 7: *dpy-13* (experimental); Lane 8: *dpy-13* (control); Lane 9: *cpg-3* (experimental); Lane 10: *cpg-3* (control); Lane 11: *cpg-2* (experimental); Lane 12: *cpg-2* (control); Lane 13: WBGene00014018 (experimental); Lane 14: WBGene00014018 (control).

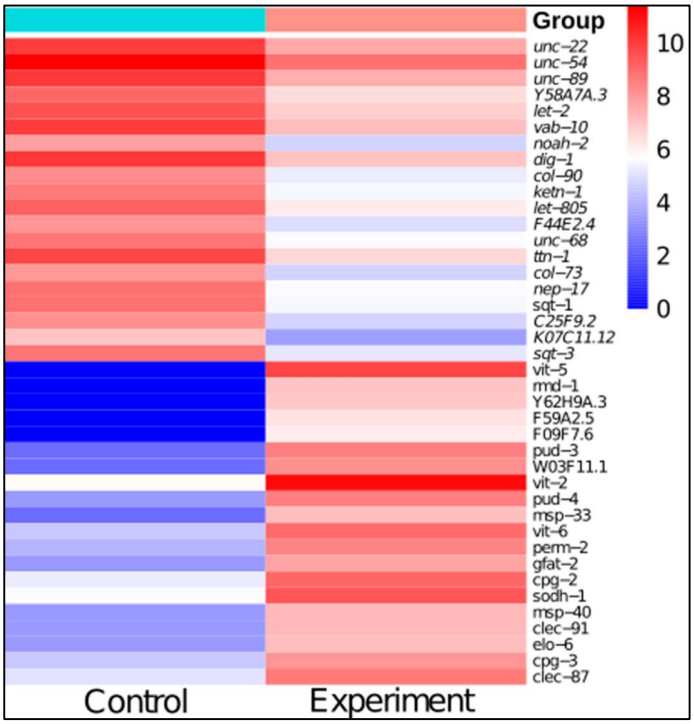

Figure S4. Heat map of DEGs in *W. somnifera*-exposed *C. elegans*. Heat map generated using the online software tool ClustVis (https://biit.cs.ut.ee/clust vis/) showing up-regulated and down-regulated genes with FDR<0.01 and log fold change '± 2'.

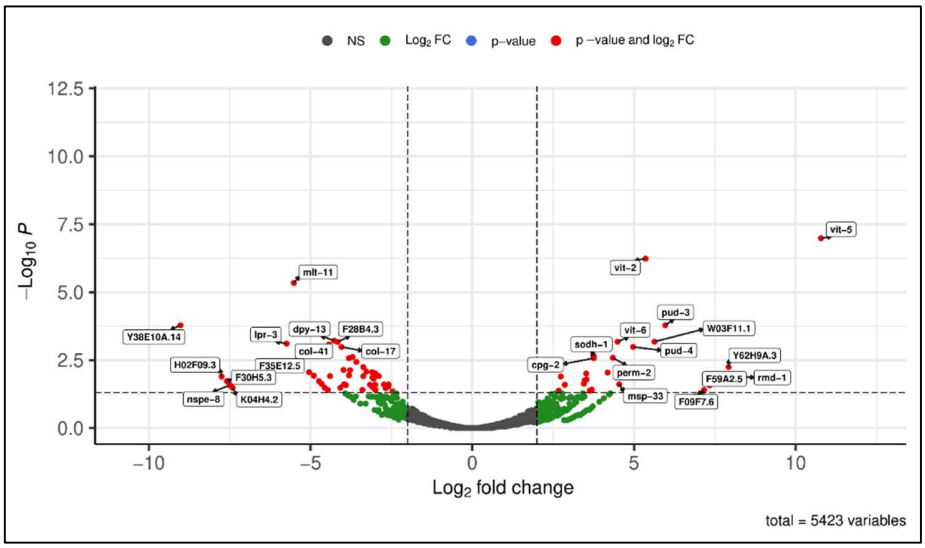

Figure S5. Volcano Plot of experimental versus control samples. Volcano plot of expressed genes of experimental culture compared to control culture. The y- axis illustrates −log 10 *p* values, and the x-axis corresponds to a log 2-fold change of gene expression between both cultures. The red points represent differently expressed genes satisfying the dual criteria of FDR≤0.01 and log fold change ≥2.

Supplement to Section 3.3. of the main text

Appendix A: Detailed discussion on important up/down-regulated genes and how their differential expression would have contributed to the observed results.

Log fold-change values of the DEG ranged from 2.74-10.78. Among the top-17 DEG, three of the upregulated genes coded for different vitellogenin lipoproteins. In *C. elegans*, the synthesis of the yolk lipoprotein (vitellogenin) occurs in the endoplasmic reticulum of the intestine, and is initiated before the worm achieves adulthood. Since vitellogenesis persists throughout and beyond the reproductive stage, lipoproteins accumulate in the passive circulatory system found between tissues (pseudocoelom) as the animal ages. While Seah et al. (2016) reported overexpression of the vitellogenin to be associated with a reduction in the lifespan of worms, our study has found an upregulation of *vit* genes in extract-exposed worms experiencing a longer life. Increased fertility observed in our study in *W. somnifera*-exposed worms corroborates well with the primary function of abundant vitellogenesis in *C. elegans* proposed by Perez and Lehner (2019), that is to support post-embryonic development and fertility, especially in harsh conditions (in our study, the ageing gnotobiotic worms faced starvation, as they were not provided any bacterial food during the whole assay). Vitellogenins are a family of yolk proteins that are the most abundant among oviparous animals. In *C. elegans*, the six vitellogenins are among the most highly expressed genes in the adult hermaphrodite intestine, which contributes towards ensuring yolk for eggs. Vitellogenins can act as an intergenerational signal mediating the influence of parental physiology on progeny. While *vit* genes are known to be important in regulating lifespan of the worms (Sornda et al., 2019), our results indicate that vitellogenins may play other important roles as well in worm physiology. Since vitellogenins are widely present across the tree of life, *W. somnifera'*s pro-health effect mediated in part through upregulation of *vit* genes can be expected to be relevant for other forms of life including humans. On the basis of sequence similarity, vitellogenins are suggested to be the ancestor of human apoB, the principal component of low density lipoprotein (Baker et al., 2019). Interestingly the three upregulated *vit* genes in our transcriptome data belong to three different groups of the vitellogenin family. Of them, the *vit*-6 is the only member of its group, and this protein was found by Nakamura et al. (1999) as a major carbonylated protein in aged *C. elegans*, with a potential role in protecting other cellular components from oxidative stress. Such oxidative stress can be believed to be experienced by the worms in our study owing to starvation (Tao et al., 2017). Vitellogenin has recently been shown to play non-nutritional roles too, by functioning as an immunocomponent factor and antioxidant (Li et al., 2017).

Upregulation of above mentioned *vit* genes gets justified in view of upregulation of multiple other genes (*cpg-2, cpg-3, ule-1* and *perm-2*) too, contributing to the common function of the hierarchical assembly of the eggshell and permeability barrier in this worm. The *C. elegans* eggshell is composed of an outer vitelline layer, a middle chitin layer, and an inner layer of chondroitin proteoglycans. Since *W. somnifera* extract promoted fertility of worms in our study, the genes contributing towards formation of the eggshell can be expected to be upregulated. Among products coded by such genes, cpg-2 is required for eggshell impermeability, and possibly an important cargo. Upregulation of *ule-1* (chitin binding domain protein) and the chondroitin

proteoglycans (*cpg-2* and *cpg-3)* can be understood in light of the fact that chitin and the *cpg-1/2* localize to the middle and inner layers of the trilaminar eggshell, respectively (Olson et al., 2012). Simultaneous upregulation of these genes can be explained by the fact that formation of the inner chondroitin proteoglycan (CPG) layer requires prior deposition of the chitin layer. The chondroitin chains play essential roles in embryonic development and vulval morphogenesis of worms. *cpg-2* is among those proteoglycans on which embryonic cell division is dependent. Owing to its expression during embryonic development and chitin-binding property, it has been suggested to have a structural role in the egg (Olson et al., 2006). Another member of the cpg group in our list of DEG, cpg-3 is also implicated in chitin and chondroitin biosynthesis and eggshell formation (Kudron et al., 2013). Upregulation of a uterine protein (ule-1) in extract-fed fertile worms can be correlated to the fact that uterine proteins turn over rapidly in young worms than old, and the extract-fed worm population was indeed displaying more 'youthful' behaviour in terms of active motility and reproduction on the day of worm collection for transcriptome purpose. Since uterine proteins are removed by egg-laying in young worms, their upregulation may be compensated by the worms through active reproduction. If that is not the case, then upregulation of *ule* genes may shorten the lifespan (Zimmerman et al., 2015). Upregulation of the *ule-1* gene in our extract-fed actively reproducing worm population matches with earlier published role of this gene, wherein it was identified in mass RNAi screens to be required for normal progeny production [(Maeda et al., 2001) and (Green et al., 2011)], and its knockdown marginally reduced the brood size. One of the upregulated genes in extract-fed worms, *perm-2* is among the key components of the vitelline layer structural scaffold, whose depletion from the scaffold can lead to a porous vitelline layer which permits soluble factors to leak through the eggshell resulting in embryonic death (González et al., 2018). perm-2 is among those proteins which are required for eggshell integrity, and its upregulation corroborates well with increased fertility of the *W. somnifera*-fed worms.

Among other upregulated genes in extract-treated worms were two *pud* genes, *pud-3* and *pud-4.* The PUD gene family comprises of six genes located next to each other on chromosome V. Pud-genes are unique to *Caenorhabditis* spp. without known orthologues in other nematodes While upregulation of other *pud* genes (*pud-1* and *pud-2*) has been reported earlier (Ding et al., 2013) in long-lived *C. elegans,* our study found different genes of the same group to be upregulated in the experimental worms. Of them, *pud-3* is known to get expressed in the nuclei of the largest hypodermal cell (hyp7) which wraps around most of the worm body, and also in the rectal gland cells, pharyngeal muscle pm3, and less frequently in the intestine and a few neuron-like cells in the head. *pud-4* gets expressed most strongly in the hyp7 nuclei and sporadically in the intestine. The nuclear localization of the PUD proteins (including those upregulated in our study) is suggested as an indication of their involvement in regulation of the transcription of the collagen genes. Slow growth of *C. elegans* after *pud-4* knockdown in worms reported by Cui et al. (2007) corroborates with our study finding the same gene getting upregulated in fast growing *W. somnifera*-exposed worms. *pud-3* and *pud-4* were downregulated in their study in worms exposed to the anthelmintic drug ivermectin. It may be thought that these *pud* genes are upregulated under favourable conditions, and downregulated under difficult conditions.

Of the top-24 DEG, four (*col-109, col-169, col-41*, and *col-17*) belonged to the *col* group of genes, and all these four were downregulated in extract-exposed worms. Downregulation of this *col* group of genes corroborates well with simultaneous downregulation of other genes (*sqt-1, sqt-3, dpy-4,* and *dpy-13*) contributing to same function e.g. cuticle collagen synthesis. These collagen genes are involved in the formation and maintenance of the worm cuticle. Collagens are essential for providing structural support and elasticity to various tissues, and hence are crucial for the integrity and protective function of the worm's outer layer. Cuticle collagens, the major cuticle component, are encoded by a large family of *col* genes and, interestingly, many of these genes express predominantly at a single developmental stage (Abete-Luzi and Eisenmann, 2018). The nematode's genome encodes 177 collagens (Sandhu et al., 2021). It is possible that the worm regulates their expression to modulate cuticle permeability as a part of its adaptive response to external environment. Outer covering of the nematode *C. elegans*, the cuticle, is synthesized five times during the worm's life by the underlying hypodermis. It is possible that since the life of worms exposed to the root extract in our study was prolonged, they reduced the pace of cuticle synthesis by downregulating expression of certain *col* genes specifically important for that particular stage of life cycle. It is possible that extract-induced longevity and pro-fertility effect might have caused the worms to undergo a rearrangement of their cuticle microstructure and permeability, may be in order to allow enhanced entry of the beneficial phytocompounds. Apical extracellular matrices (aECMs) are complex extracellular compartments that form important interfaces between animals and their environment. In the adult *C. elegans* cuticle, layers are connected by regularly spaced columnar structures (Adams et al., 2023). It is possible that the extract would have triggered remodelling of this precise aECM patterning at the nanoscale. While multiple *col* genes were downregulated in extract-treated worms, since not much is known about role of these genes in maintaining the structure or barrier function of the cuticle and the cuticle permeability, it is difficult to discuss how precisely downregulation of these genes can be correlated to enhanced lifespan and fertility in extract-fed worms.

In total, 8 genes contributing towards collagen synthesis were downregulated in our experimental worm population. This might have led to some degree of collagen restructuring, which in turn may have dramatic effects on organism's morphology. Among collagen synthesis-associated genes other than the *col* genes found among our DEG, the *sqt-1* plays a unique role in determining the structure of the cuticle and the morphology of the animal. This gene has been reported to encode a collagen, which is critical for morphogenesis of *C. elegans* (Kramer et al., 1988). Other genes belonging to same group, *sqt-3* codes for an early cuticle collagen. Its downregulation may have slowed down the formation of the basal striated layer of the L1 cuticle, which forms only after embryo elongation (Birnbaum et al., 2023). The C terminus of collagen sqt-3 has been reported for its complex and essential role in nematode collagen assembly (Novelli et al., 2006). Though *sqt-3* is recognized mainly as a component of the cuticle, but other important roles of it have also been indicated. For example, it has been shown to direct anterior–posterior migration of the Q Neuroblasts in *C. elegans* (Lang and Lundquist, 2021). Two more genes coding for cuticle collagen components, *dpy-13* and *dpy-4* were also downregulated in extract-treated worms. Of them, *dpy-13* is among those having specific roles in the formation of the exoskeleton (Nyström et al., 2002), and it has also been identified as a collagen gene influencing the nematode

body shape (von Mende et al., 1988) Extract-treated worms in our study experiencing downregulation of *dpy-4* can still be believed to have no cuticle abnormality, as *dpy-4* non-expressing mutant of *C. elegans* were shown to possess normal ultrastructure of the cuticle similar to wild type control animals. The *dpy-4* RNAi animals were shown to bear a periodic arrangement of annuli and furrows, without any irregular indentations (Sandhu et al., 2021).

Two *unc* genes, *unc-52* and *unc-68* were downregulated in extract-exposed worm population. The *unc-52* gene of *C. elegans* codes for a homologue of the basement membrane heparan sulfate proteoglycan perlecan, which was shown to affect gonadal leader cell migrations in hermaphrodite worms through alterations in growth factor signalling. *unc-52* has been proposed to play dual roles in *C. elegans* larval development in the maintenance of muscle structure, as well as, the regulation of growth factor-like signalling pathways (Merz et al., 2003). Downregulation of *unc-52* can be expected to have altered the formation or maintenance of the muscle myofilament lattice (Rogalski et al., 2001). Another downregulated gene, *unc-68* codes for a ryanodine receptor involved in regulating worm body-wall muscle contraction. Ryanodine receptors are not believed to be essential for excitation-contraction coupling in nematodes, but they do act to amplify a calcium signal to the extent sufficient for contraction. Though *unc-68* mutants were reported to be somewhat defective with respect to motility and pharyngeal pumping (Maryon et al., 1996), its downregulation in our extract-exposed worms did not have any negative effect on motility. In fact, they were more actively motile than control worms (Figure 2A; Videos S1-S2). Any possible effect of *unc-68* downregulation on pharyngeal pumping is not of much relevance to our study, as we did not provide any solid (e.g. bacterial cells) food to the worms during the assay. Higher proficiency of *unc-68* mutants with respect to egg laying reported by Maryon et al. corroborates with our observation of increased fertility in extract-exposed worms.

Fold-change wise, the third most differently expressed gene in extract-fed worms was *rmd-1*, which codes for a microtubule-associated protein, having function in chromosome segregation in *C. elegans*. Importance of the upregulation of this regulator of microtubule dynamics in *W. somnifera*-exposed worms can be understood from the fact that depletion of this protein can induce severe defects in chromosome segregation. Relevance of this result can be visualized better in light of the fact that human homologues of *rmd-1* also bind microtubules, suggesting a function for these proteins in chromosome segregation during mitosis in other organisms as well (Oishi et al., 2007). Non-expression of *rmd-1* leads to defects in chromosome segregation and microtubule outgrowth. It can be said that in addition to regulating microtubule outgrowth, *rmd-1* has specific functions in the execution of proper chromosome segregation, may be by preventing abnormal attachments. *rmd-1,2,3,6* is a family of homologous proteins conserved between humans and *C. elegans,* and perhaps *rmd-1* is the most important of them all, as paternal mitochondria from an *rmd-2, rmd-3*, *rmd-6* triple mutant were reported to be properly positioned in the *C. elegans* zygote, with a possible explanation that *rmd-1* carries out all the essential functions of this gene family (Juanico et al., 2021).

The seventh top differently expressed gene in experimental worm population was that coding for a lipocalinprotein *lpr-3*, which was downregulated 5.74-fold. Lipocalins in general are

required for apical extracellular matrix organization and remodelling in *C. elegans*. *lpr-3* has a distinct function in precuticular glycocalyx of developing external epithelia. Experimental worms under the influence of root extract experiencing a downregulation of this gene can be expected to have altered phenotype with respect to maintenance of a passable excretory duct lumen, eggshell degradation, shedding of cuticle during molting, cuticle barrier function, and clearance and remodelling of apical extracellular matrix. Its altered expression would have affected multiple aspects of later cuticle structure or molting in worms. *lpr-3* contributes towards maintenance of a uniform duct lumen diameter, as well as, tube patency during lumen elongation and narrowing. Since LPR-3 is present within a juvenile glycocalyx layer, and the connection between this layer and the mature cuticle is weakened during molting, its downregulation would have affected molting in extract-fed worms. Lipocalins are believed to exert direct effects on aECM lipid, metalloproteinase, and/or glycoprotein content, and thereby affect molting and hatching (Forman-Rubinsky et al., 2017). Downregulation of *lpr-3* in long-lived fertile worms in the extract-fed wells becomes more relevant considering that accumulation of this proteins needs to be prevented for ensuring proper localization of the Zona Pellucida domain protein *let-653* within the vulva precuticle (Cohen et al., 2021). Downregulation of *lpr-3* makes more sense when looked together with downregulation of another molting factor (*mlt-11*) in our long-lived worms. Both these genes are among top-10 differently expressed genes. *mlt-11* is a molting factor, and a putative protease inhibitor in *C. elegans*, necessary for embryogenesis, that localizes to lysosomes and the cuticle. It has been demonstrated to be a secreted protein, which localizes in the cuticle and in a punctate pattern reminiscent of lysosome (Clancy et al., 2023). *mlt-11* is proposed to be acting in the aECM to coordinate remodeling and timely ecdysis. Its downregulation can be expected to influence developmental pace, motility, apolysis, and cuticle structure (Ragle et al., 2022).

Another among top-downregulated genes was *irg-5*, which is an immune effector known to be induced in response to bacterial pathogen attack, as well as by exposure to immunostimulatory compounds (Anderson et al., 2019). Its downregulation may not have any negative effect on the worm lifespan as knockdown of *irg-5* was reported not to shorten the lifespan of *C. elegans* grown on *E. coli* OP50 (Peterson et al., 2019).

References

(a) Abete-Luzi P, Eisenmann DM. Regulation of C. elegans L4 cuticle collagen genes by the heterochronic protein LIN-29. *Genesis*. 2018 ;56(5). https://doi.org/10.1002/dvg.23106

(b) Adams JR, Pooranachithra M, Jyo EM, Zheng SL, Goncharov A, Crew JR, Kramer JM, Jin Y, Ernst AM, Chisholm AD. Nanoscale patterning of collagens in C. elegans apical extracellular matrix. *Nature Communications*. 2023;14(1):7506. https://doi.org/10.1038/s41467-023-43058-9

(c) Anderson SM, Cheesman HK, Peterson ND, Salisbury JE, Soukas AA, Pukkila-Worley R. The fatty acid oleate is required for innate immune activation and pathogen defense in Caenorhabditis elegans. *PLoS Pathogens*. 2019;15(6):e1007893. https://doi.org/10.1371/journal. ppat.1007893

(d) Baker ME. Is vitellogenin an ancestor of apolipoprotein B-100 of human low-density lipoprotein and human lipoprotein lipase?. *Biochemical Journal*. 1988;255(3):1057-60. https://doi.org/10.1042/bj2551057
(e) Birnbaum SK, Cohen JD, Belfi A, Murray JI, Adams JR, Chisholm AD, Sundaram MV. The proprotein convertase BLI-4 promotes collagen secretion during assembly of the Caenorhabditis elegans cuticle. *bioRxiv.* 2023 https://doi.org/10.1101/2023.06.06.542650
(f) Clancy JC, Vo AA, Myles KM, Levenson MT, Ragle JM, Ward JD. Experimental considerations for study of C. elegans lysosomal proteins. *G3: Genes, Genomes, Genetics.* 2023;13(4):jkad032. https://doi.org/10.1093/g3journal/jkad032
(g) Cohen JD, Cadena del Castillo CE, Serra ND, Kaech A, Spang A, Sundaram MV. The Caenorhabditis elegans Patched domain protein PTR-4 is required for proper organization of the precuticular apical extracellular matrix. *Genetics*. 2021;219(3):iyab132. DOI: 10.1093/genetics/iyab132
(h) Cui Y, McBride SJ, Boyd WA, Alper S, Freedman JH. Toxicogenomic analysis of Caenorhabditis elegans reveals novel genes and pathways involved in the resistance to cadmium toxicity. *Genome Biology*. 2007; 8(6):R122. https://doi.org/10.1186/gb-2007-8-6-r122
(i) Ding YH, Du YG, Luo S, Li YX, Li TM, Yoshina S, Wang X, Klage K, Mitani S, Ye K, Dong MQ. Characterization of PUD-1 and PUD-2, two proteins up-regulated in a long-lived daf-2 mutant. *PLoS One*. 2013;8(6):e67158. https://doi.org/10.1371/annotation/6b155146-de73-4733-83b0-62224d84717e
(j) Forman-Rubinsky R, Cohen JD, Sundaram MV. Lipocalins are required for apical extracellular matrix organization and remodeling in Caenorhabditis elegans. *Genetics.* 2017;207(2):625-42. https://doi.org/10.1534/genetics.117.300207
(k) González DP, Lamb HV, Partida D, Wilson ZT, Harrison MC, Prieto JA, Moresco JJ, Diedrich JK, Yates III JR, Olson SK. CBD-1 organizes two independent complexes required for eggshell vitelline layer formation and egg activation in C. elegans. *Developmental Biology*. 2018;442(2):288-300. https://doi.org/10.1016/j.ydbio.2018.08.005
(l) Green RA, Kao HL, Audhya A, Arur S, Mayers JR, Fridolfsson HN, Schulman M, Schloissnig S, Niessen S, Laband K, Wang S. A high-resolution C. elegans essential gene network based on phenotypic profiling of a complex tissue. *Cell*. 2011;145(3):470-82. doi: 10.1016/j.cell.2011.03.037
(m) Juanico IY, Meyer CM, McCarthy JE, Gong T, McNally FJ. Paternal mitochondria from an rmd-2, rmd-3, rmd-6 triple mutant are properly positioned in the C. elegans zygote. *Micropublication Biology*. 2021;2021. https://doi.org/10.17912%2Fmicropub.biology.000422
(n) Kramer JM, Johnson JJ, Edgar RS, Basch C, Roberts S. The sqt-1 gene of C. elegans encodes a collagen critical for organismal morphogenesis. *Cell*. 1988;55(4):555-65. https://doi.org/10.1016/0092-8674(88)90214-
(o) Kudron M, Niu W, Lu Z, Wang G, Gerstein M, Snyder M, Reinke V. Tissue-specific direct targets of Caenorhabditis elegans Rb/E2F dictate distinct somatic and germline programs. *Genome Biology*. 2013;14:1-7.
(p) Lang AE, Lundquist EA. The Collagens DPY-17 and SQT-3 Direct Anterior–Posterior Migration of the Q Neuroblasts in C. elegans. *Journal of Developmental Biology*. 2021;9(1):7. https://doi.org/10.3390/jdb9010007

(q) Li H, Zhang S. Functions of vitellogenin in eggs. Oocytes: *Maternal Information and Functions*. 2017:389-401. https://doi.org/10.1007/978-3-319-60855-6_17
(r) Maeda I, Kohara Y, Yamamoto M, Sugimoto A. Large-scale analysis of gene function in Caenorhabditis elegans by high-throughput RNAi. *Current Biology*. 2001; 11(3):171–6. https://doi.org/10.1016/S0960-9822(01)00052-5
(s) Maryon EB, Coronado R, Anderson P. unc-68 encodes a ryanodine receptor involved in regulating C. elegans body-wall muscle contraction. *The Journal of Cell Biology*. 1996;134(4):885-93.
(t) Merz DC, Alves G, Kawano T, Zheng H, Culotti JG. UNC-52/perlecan affects gonadal leader cell migrations in C. elegans hermaphrodites through alterations in growth factor signaling. *Developmental Biology*. 2003;256(1):174-87. DOI:10.1016/S0012-1606(03)00014-9
(u) Nakamura A, Yasuda K, Adachi H, Sakurai Y, Ishii N, Goto S. Vitellogenin-6 is a major carbonylated protein in aged nematode, Caenorhabditis elegans. *Biochemical and Biophysical Research Communications.* 1999;264(2):580-3. https://doi.org/10.1006/bbrc.1999.1549
(v) Novelli J, Page AP, Hodgkin J. The C terminus of collagen SQT-3 has complex and essential functions in nematode collagen assembly. *Genetics*. 2006;172(4):2253-67. DOI: 10.1534/genetics.105.053637
(w) Nyström J, Shen ZZ, Aili M, Flemming AJ, Leroi A, Tuck S. Increased or decreased levels of Caenorhabditis elegans lon-3, a gene encoding a collagen, cause reciprocal changes in body length. *Genetics.* 2002;161(1):83-97. https://doi.org/10.1093/genetics/161.1.83
(x) Oishi K, Okano H, Sawa H. RMD-1, a novel microtubule-associated protein, functions in chromosome segregation in Caenorhabditis elegans. *The Journal of Cell Biology*. 2007;179(6):1149-62. http://www.jcb.org/cgi/doi/10.1083/jcb.200705108
(y) Olson SK, Bishop JR, Yates JR, Oegema K, Esko JD. Identification of novel chondroitin proteoglycans in Caenorhabditis elegans: embryonic cell division depends on CPG-1 and CPG-2. *The Journal of Cell Biology*. 2006;173(6):985-94. https://doi.org/10.1083/jcb.200603003
(z) Olson SK, Greenan G, Desai A, Müller-Reichert T, Oegema K. Hierarchical assembly of the eggshell and permeability barrier in C. elegans. *Journal of Cell Biology*. 2012;198(4):731-48. https://doi.org/10.1083/jcb.201206008
(aa) Perez MF, Lehner B. Vitellogenins-yolk gene function and regulation in Caenorhabditis elegans. *Frontiers in Physiology*. 2019;10:471381. https://doi.org/10.3389/fphys.2019.01067
(bb) Peterson ND, Cheesman HK, Liu P, Anderson SM, Foster KJ, Chhaya R, Perrat P, Thekkiniath J, Yang Q, Haynes CM, Pukkila-Worley R. The nuclear hormone receptor NHR-86 controls anti-pathogen responses in C. elegans. *PLoS Genetics*. 2019;15(1):e1007935. https://doi.org/10.1371/journal. pgen.1007935
(cc) Ragle JM, Levenson MT, Clancy JC, Vo AA, Pham V, Ward JD. The conserved, secreted protease inhibitor MLT-11 is necessary for C. elegans molting and embryogenesis. *bioRxiv*. 2022:2022-06. https://doi.org/10.1101/2022.06.29.498124
(dd) Rogalski TM, Mullen GP, Bush JA, Gilchrist EJ, Moerman DG. UNC-52/perlecan isoform diversity and function in Caenorhabditis elegans. *Biochemical Society Transactions*. 2001;29(2):171-6.

(ee) Sandhu A, Badal D, Sheokand R, Tyagi S, Singh V. Specific collagens maintain the cuticle permeability barrier in Caenorhabditis elegans. *Genetics*. 2021;217(3):iyaa047. https://doi.org/10.1093/genetics/iyaa047

(ff) Seah NE, de Magalhaes Filho CD, Petrashen AP, Henderson HR, Laguer J, Gonzalez J, Dillin A, Hansen M, Lapierre LR. Autophagy-mediated longevity is modulated by lipoprotein biogenesis. *Autophagy*. 2016;12(2):261-72. https://doi.org/10.1080/15548627.2015.1127464

(gg) Sornda T, Ezcurra M, Kern C, Galimov ER, Au C, de la Guardia Y, Gems D. Production of YP170 vitellogenins promotes intestinal senescence in Caenorhabditis elegans. *The Journals of Gerontology: Series A*. 2019;74(8):1180-8. https://doi.org/10.1093/gerona/glz067

(hh) Tao J, Wu QY, Ma YC, Chen YL, Zou CG. Antioxidant response is a protective mechanism against nutrient deprivation in C. elegans. *Scientific Reports*. 2017;7(1):43547. DOI: 10.1038/srep43547

(ii) von Mende N, Bird DM, Albert PS, Riddle DL. dpy-13: a nematode collagen gene that affects body shape. *Cell.* 1988;55(4):567-76. https://doi.org/10.1016/0092-8674(88)90215-2

(jj) Zimmerman SM, Hinkson IV, Elias JE, Kim SK. Reproductive aging drives protein accumulation in the uterus and limits lifespan in C. elegans. *PLoS Genetics*. 2015;11(12):e1005725. DOI: 10.1371/journal.pgen.1005725

Legend to Supplementary Videos

We investigated the effect of the hydroalcoholic extract of *Withania somnifera* root on lifespan and healthspan of the model worm *Caenorhabditis elegans*. Positive effect of the extract on worm's lifespan, motility, and fertility can be visualized in the supplementary videos listed below:
Video S1: (control well) A worm in M9 buffer (devoid of plant extract) captured at 7th day. S1a and S1b are two different worms from two different wells.
Video S2: Worm population in extract (600 µg/mL)-supplemented media, captured on the 7th day. Actively moving progenies are visible (which were absent in corresponding control video 'A'). Adult worms too can be seen exhibiting movement better than their counterparts in 'control' wells. Comparative assessment of video A vs. B reveals abnormal body movement and smaller body size in control worms, as against bigger body size and normal movement in extract-fed worms.
Video S3: Control worm population at 12th day, whereby ~100% worms were dead, as evident from lack of movement. Morphological damage can also be seen.
Video S4: Extract-fed worms captured on the 12th day. Actively moving adult as well as progeny worms can be seen. Morphology of the parent worms (i.e. those with whom experiment started) seems normal.

All these videos were captured at the end of the 7th or 12th day of incubation, i.e., the days on which the control population exhibited ~50% and ~100% death, respectively. Videos were captured using a Magnus Camera (5.1 MP) attached to a Labomed Vision 2000 (halogen light source) binocular microscope (4X objective).